The Astrophysical Journal, 812:2 (8pp), 2015 October 10 doi:10.1088/0004-637X/812/1/2
© 2015. The American Astronomical Society. All rights reserved.

PUSHING THE LIMITS, EPISODE 2: K2 OBSERVATIONS OF EXTRAGALACTIC RR LYRAE STARS IN THE DWARF GALAXY LEO IV

L. Molnár[1], A. Pál[1,2], E. Plachy[1], V. Ripepi[3], M. I. Moretti[4,5], R. Szabó[1], and L. L. Kiss[1,6,7]
[1] Konkoly Observatory, Research Centre for Astronomy and Earth Sciences, Hungarian Academy of Sciences, H-1121 Budapest, Konkoly Thege Miklós út 15-17, Hungary; molnar.laszlo@csfk.mta.hu
[2] Eötvös Loránd Tudományegyetem, H-1117 Pázmány Péter sétány 1/A, Budapest, Hungary
[3] INAF—Osservatorio Astronomico di Capodimonte, Via Moiariello 16, I-80131 Naples, Italy
[4] INAF—Osservatorio Astronomico di Bologna, via Ranzani 1, I-40127 Bologna, Italy
[5] Scuola Normale Superiore di Pisa, piazza dei Cavalieri 7, I-56126 Pisa, Italy
[6] Gothard-Lendület Research Team, H-9704 Szombathely, Szent Imre herceg út 112, Hungary
[7] Sydney Institute for Astronomy, School of Physics A28, University of Sydney, NSW 2006, Australia
Received 2015 July 15; accepted 2015 August 21; published 2015 October 2

ABSTRACT

We present the first observations of extragalactic pulsating stars in the K2 ecliptic survey of the *Kepler* space telescope. The variability of all three RR Lyrae stars in the dwarf spheroidal galaxy Leo IV was successfully detected, at a brightness of $Kp \approx 21.5$ mag, from data collected during Campaign 1. We identified one modulated star and another likely Blazhko candidate with periods of 29.8 ± 0.9 days and more than 80 days, respectively. EPIC 210282473 represents the first star beyond the Magellanic Clouds for which the Blazhko period and cycle-to-cycle variations in the modulation were unambiguously measured. The photometric [Fe/H] indices of the stars agree with earlier results that Leo IV is a very metal-poor galaxy. Two out of the three stars blend with brighter background galaxies in the K2 frames. We demonstrate that image subtraction can be reliably used to extract photometry from faint confused sources, which will be crucial not only for the K2 mission but also for future space photometric missions.

Key words: methods: observational – stars: variables: RR Lyrae – techniques: photometric

Supporting material: machine-readable table

1. INTRODUCTION

Kepler has provided incredible results on extrasolar planets and planetary systems, as well as on stellar astrophysics. The space telescope was designed to be the most precise photometer ever built for the purpose of detecting the transits of numerous small planets (Borucki et al. 2010). To achieve this goal, the original *Kepler* mission focused almost exclusively on the Galactic stellar population, approximately 170,000 targets, within the Lyra–Cygnus field. However, after the failure of two reaction wheels, the telescope permanently lost its ability to maintain its original altitude. Soon, a new mission, called K2, was initiated to save the otherwise healthy and capable space telescope (Howell et al. 2014). Since then, *Kepler* has been observing in shorter, 75-day campaigns along the Ecliptic to balance the radiation pressure from the Sun.

The new fields opened the possibility of extending the capabilities of *Kepler* into new areas, and so we set out to explore the limits of the K2 mission. Molnár et al. (2015) investigated the first observations of field RR Lyrae stars. Szabó et al. (2015) and Pál et al. (2015) showed that *Kepler* can be used for Solar System research, including the detection of main-belt asteroids and trans-neptunian objects (TNOs). In this paper, we continue this work, expanding the reach of *Kepler* toward extragalactic pulsating stars. The three RR Lyrae stars in the galaxy Leo IV are the first non-cataclysmic stellar targets *Kepler* ever detected outside the Galaxy. We note in passing that the space telescope already observed four supernovae during the original mission (Olling et al. 2015).

Leo IV is one of the small and faint dwarf spheroidal galaxies around the Milky Way that were recently discovered with the help of the Sloan Digital Sky Survey, with a mass and luminosity of $M = (1.4 \pm 1.5) \cdot 10^6\, M_\odot$ and $M_V = -5.1 \pm 0.6$ mag (Belokurov et al. 2007; Simon & Geha 2007). It is located at a heliocentric distance of 154 ± 5 kpc, and has a half-light radius of 3.3 arcmin translating to a physical size of 160 pc (Moretti et al. 2009). Most of the stars in Leo IV are older than 12 Gyr, although another brief episode of star formation likely occurred 1–2 Gyr ago (Sand et al. 2010). The galaxy is very metal-poor: different studies determined the average metallicity to be around $\langle [Fe/H] \rangle = -2.3$ (Simon & Geha 2007; Sand et al. 2010) or possibly as low as $\langle [Fe/H] \rangle = -2.58$ (Kirby et al. 2008). The galaxy was also surveyed by Moretti et al. (2009), who discovered four variable stars, three fundamental-mode RR Lyrae (RRab), and a single SX Phe pulsator.

RR Lyrae stars are ubiquitous in all nearby galaxies and have been even detected beyond the Local Group (Da Costa et al. 2010), but our knowledge decreases with distance. Our closest neighbors, the Magellanic Clouds and the Sagittarius dwarf with its stellar stream have been surveyed extensively, both in terms of stars and temporal coverage, thanks to the MACHO and OGLE programs (see, for example, Alcock et al. 1996; Soszynski et al. 2009, 2010, 2014). However, studies of other galaxies, especially those beyond 80–100 kpc, are based on a smaller amount of data. These observations are usually aimed at distance determination and population studies.

Extragalactic surveys have their limitations, however. Multiple studies have revealed several candidate Blazhko stars. Stetson et al. (2014), for example, identified 24 stars out of 194 RR Lyrae stars in Leo I with signs of amplitude variation, and we know one candidate in M31 as well (Brown et al. 2004). These low occurrences are likely just lower limits: we now know that about 50% of RRab stars are modulated in the Milky

Table 1
Summary of the K2 Observations of the RR Ly Targets in the Dwarf Galaxy Leo IV

Object	Mask (px)	R.A. (J2000)	decl. (J2000)	V (mag)	ID
210282472	15 × 14	$11^h32^m55\overset{s}{.}8$	$-0°33'29\overset{''}{.}4$	21.46	V2
210282473	15 × 13	$11^h32^m59\overset{s}{.}2$	$-0°34'03\overset{''}{.}6$	21.47	V1
210282474	14 × 14	$11^h33^m36\overset{s}{.}6$	$-0°38'43\overset{''}{.}3$	21.52	V3

Note. IDs refer to the identifications given by Moretti et al. (2009).

Way (Jurcsik et al. 2009; Benkő et al. 2014). However, in order to determine accurate occurrence rates and modulation periods of Blazhko stars, several weeks of intensive observations are usually required, and thus unambiguous detections have not yet been made. Also, data from *Kepler* revealed that continuous observations are the key to detecting any cycle-to-cycle variations—another feature that earlier studies lacked (Szabó et al. 2010). Therefore, we set out to gather the first extended, uninterrupted observations from extragalactic pulsating stars with the help of K2.

2. OBSERVATIONS AND DATA REDUCTION

Leo IV fell into the field of view of the first scientific campaign (C1) of the K2 mission and was observed between 2014 May 30 and August 21, corresponding to Barycentric Julian Day (BJD) 2456808.18–2456890.33. We requested observations of the 3 RR Lyrae variables and the 16 brightest giant stars in the galaxy through K2 Guest Observer proposal GO1019 in long cadence mode, with an integration time of 29.4 minutes. We estimated the maximum brightness of the RR Lyrae stars to be around $Kp = 21$–21.2 mag in the *Kepler* passband, leading to a precision of a few tenths of a magnitude per long cadence data point. At that time, the much fainter SX Phe star ($V = 23.0$ mag) seemed to be beyond the capabilities of *Kepler*, and so we did not include it in the proposal, although recent experiences with the similarly faint TNO 2002 GV_{31} suggest that we also could have detected its variation (Pál et al. 2015). In this paper, we focus on the three RR Lyrae stars from the sample. The summary of their observation parameters is shown in Table 1.

For all of the tasks described below, we exclusively employed the utilities shipped within Fitsh[8] (Pál 2012). Fitsh is a lightweight, yet comprehensive, fully open source astronomical data reduction and analysis software package. It is comprised of a collection of standalone binary programs that are utilized through various UNIX shell scripts. The accurate photometric time series for these three extragalactic Leo IV RR Lyr targets were obtained as follows. The image scale of *Kepler* is $3\overset{''}{.}98$/px, and the point-spread functions are at least 3–5 px wide, which leads to confusion in nearby sources. Although Leo IV is sparse enough to be resolved even with *Kepler*, two out of the three RR Lyr targets were extremely close to bright background galaxies (i.e., nearly within a pixel, see Figures 1 and 2), and thus accurate photometry could only be performed using image subtraction techniques. Since the pointing jitter of *Kepler* in the K2 mission was in the range of a pixel, the individual frames had to be adjusted to the same reference system before

[8] http://fitsh.szofi.net/

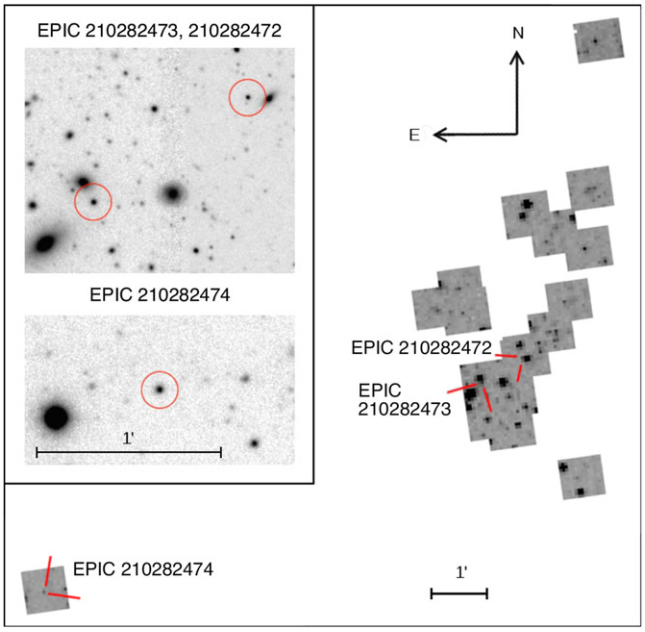


Figure 1. K2 target pixel masks covering parts of Leo IV. The three RR Lyrae stars are indicated. The insert shows the high-resolution deep imagery obtained by combining data from the William Herschel Telescope, the Isaac Newton Telescope, and the Southern Astrophysical Research telescope, collected by Moretti et al. (2009). Red circles represent the apertures used in the reduction of the K2 data (see Figure 2).

performing any kind of differential image analysis. In order to precisely estimate the shifts and rotations between the (subsequent) frames, we involved additional K2 frames since the raw K2 data do not include a frame-by-frame centroid coordinate. These additional 14 fields were the target pixel files of EPIC 201424914, 201430029, and the 12 stamps having an identifier between 210282475 and 210282486, all from the GO1019 proposal (where EPIC refers to the K2 Ecliptic Plane Input Catalog). These 3 + 14 stamps were combined into a single image and the foreground stars were used to obtain precisely the transformation between these images (Figure 1).

Since the K2 mission observes along the ecliptic plane in an approximately 10°-wide area, the background of these observations also varies gradually due to the increasing amount of zodiacal light throughout the campaign. Hence, prior to any differential analysis, the background must also be subtracted. Luckily, the fields containing the 3 RR Lyr targets, as well as the additional 14 stamps, were not crowded and the background can simply be determined by considering the median of all of the observed pixel values.

After the frames were registered to the same reference system and the background was subtracted accordingly, we chose every 20th image to obtain the median-averaged master frame used as a reference for image subtraction. Since the number of stars with a good signal-to-noise ratio in these frames was insufficient and the instrument does not show any significant variation in its point-spread function, we did not perform any cross-convolution between the adjusted images. This procedure also simplified the evaluation of the photometry, and hence it was not necessary to perform photometry on convolved apertures (Pál 2009). Therefore, the final fluxes were obtained as the sum of the flux in the

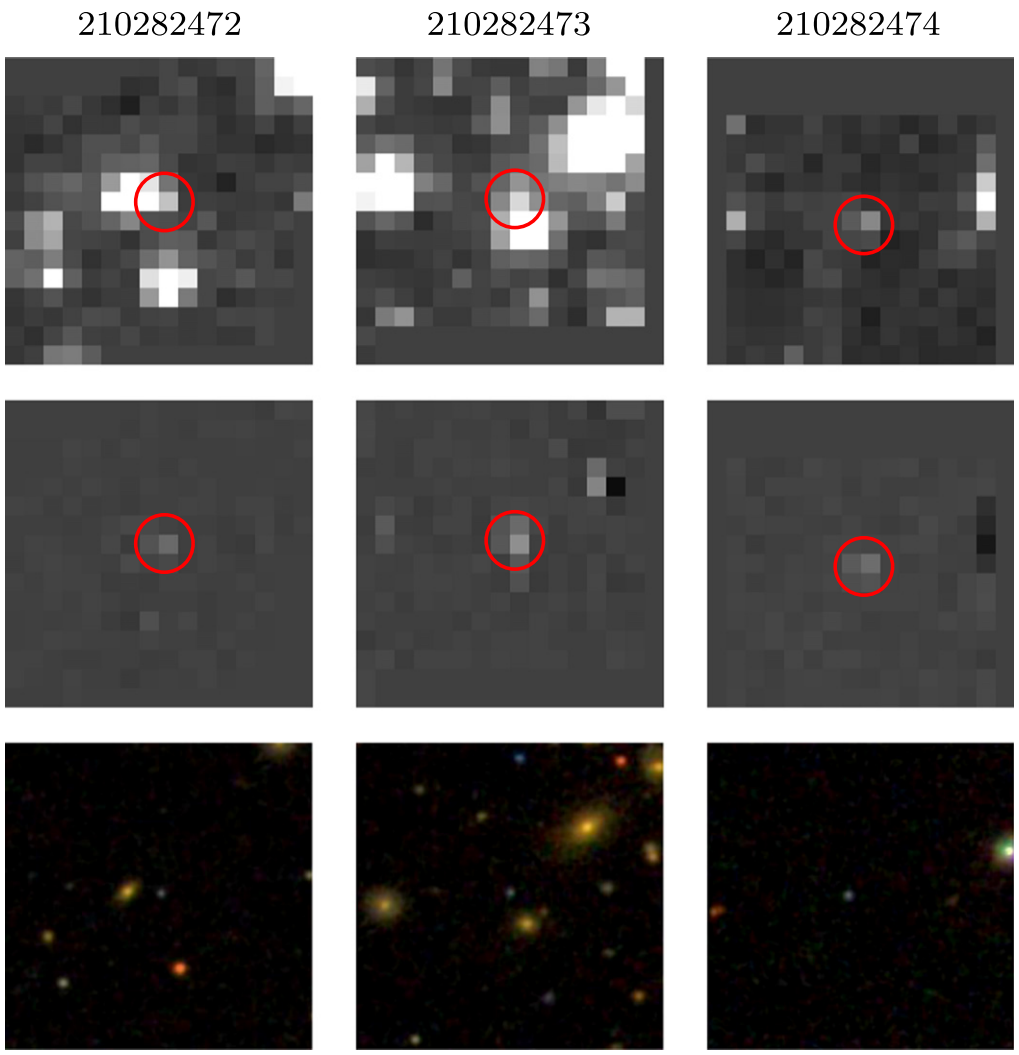


Figure 2. Image stamps showing the vicinity of the K2 extragalactic RR Lyrae targets 210282472, 210282473, and 210282474. The first row shows the stamps on the master median-combined image used in the process of differential photometry. The second row shows stamps created as the average of roughly a dozen differential images taken at the brightest phase of the RR Lyr oscillations. The photometric aperture with an $r = 1.5$ px radius used in the procedure is shown as a red circle. Stamps in the third row show the respective SDSS DR9 images. All of these stamps cover an area of $64'' \times 64''$ on the sky, equivalent to 16×16 *Kepler* pixels.

subtracted frame and in the master frame, i.e., $F_i = F_{i,\mathrm{subtr}} + F_{\mathrm{master}}$. For these flux estimates, we used simple aperture photometry with an aperture radius of $r = 1.5$ px (Figure 2). However, we should note that the reference flux on the master frame can only be estimated with an additional systematic uncertainty in the case of the confused sources (210282472 and 210282473). Namely, we compared the peak pixel values on the stellar sources with the fluxes obtained using an aperture of $r = 1.5$ px. The ratio of these two numbers aids the estimation of the reference flux in the case of confused sources as well, and we found that the systematic uncertainty of this method is in the range of 2%–3% for these sources. Due to the nature of the differential photometry, this kind of systematics yields a systematic amplification in the variability amplitudes. The random errors in the photometric fluxes have been estimated using the photon noise derived from an instrumental gain of 113.3 e^-/ADU as well as the standard deviation of the background pixels near the target sources. Due to the differential processing, this latter component also includes the photon noise of the nearby confusing sources.

3. LIGHT-CURVE ANALYSIS

Once the raw light curves were obtained, we removed the outliers from the light curves with a sigma-clipping algorithm. We subtracted an initial Fourier fit from the light curves, clipped the residual at the 3σ levels three consecutive times, and then restored the original signal.

Finally, we applied Fourier filtering to remove the slow variations. The photometry of these faint targets is very sensitive to variations in the background flux level. Even the best raw light curves we extracted contained additional variations up to 0.1–0.2 mag in the last 10–20 days of data. However, a simple high-pass frequency filter would remove any modulation signal along with the low-frequency noise. So instead we removed all of the low-frequency components below 0.5 day^{-1} that were stronger than 10 mmag and not connected to any potential modulation frequencies. The final light curves are displayed in the left panels of Figure 3. The right panels show the folded light curves, along with the binned phase curves.

The increasing background from the zodiacal light lowered the photometric accuracy of individual data points toward the

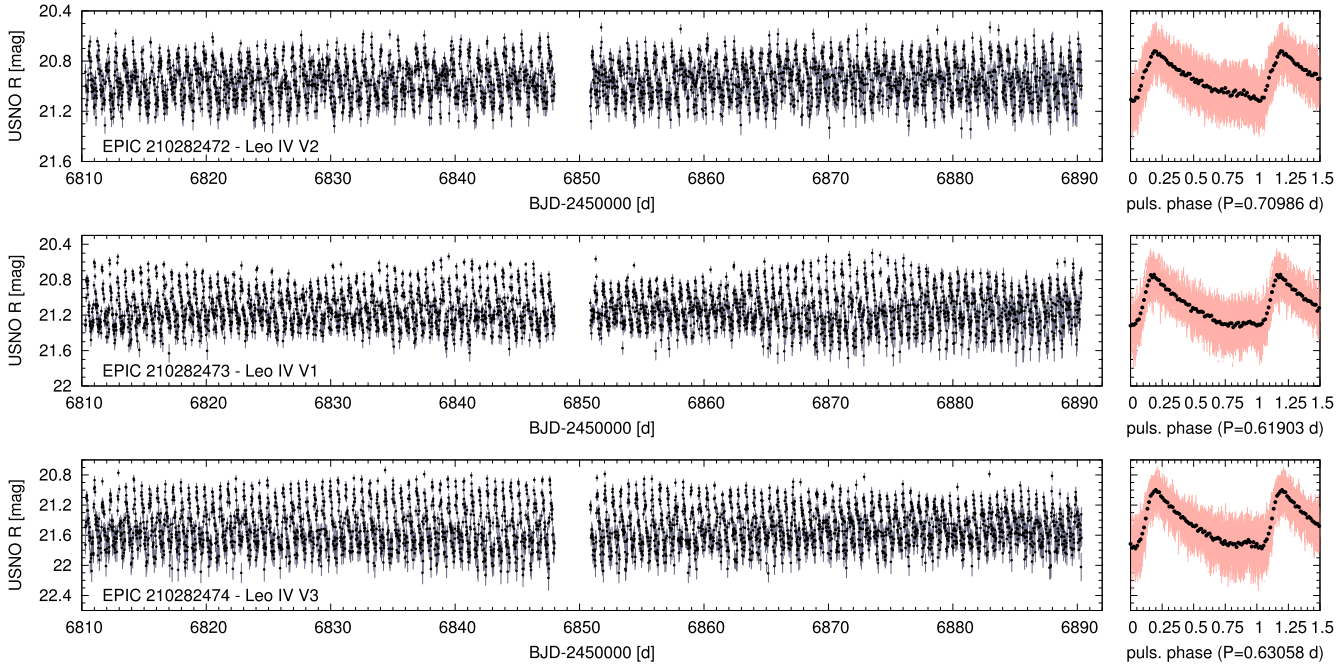


Figure 3. Light curves of the three RR Lyrae stars. Left panels: light curves after outlier removal and Fourier filtering. Note the variable amplitude of EPIC 210282473 in the middle panel. Designations from Moretti et al. (2009) are also indicated. The right panels show the folded light curves (pink dots and lines) and the binned phase curves (black points). We used 75 bins per pulsation period for each star.

end of the campaign. The accuracy of a single LC point was similar for EPIC 210282472 and 210282473: 0.050–0.055 mag at the beginning and 0.078–0.092 mag during the last days of the measurements. The errors are somewhat higher for the unblended star EPIC 210282474, starting from 0.087 mag and reaching 0.107 mag at the end of the campaign. 210282472 and 210282473 also appear to be brighter than 210282474 by 0.50 and 0.34 mag, respectively. As mentioned, the main component of this difference comes from the uncertainty of the zero-point determination for the confused sources. Similar differences appear in the peak-to-peak amplitudes, which are lowered to 0.4 and 0.6 mag for 210282472 and 210282473, compared to 0.94 mag for 210282474. In contrast, Moretti et al. (2009) found the amplitudes to be quite similar: 0.64, 0.73, and 0.65 mag in the V band, respectively. All of these differences between EPIC 210282474 and the other two stars indicate that the confusing sources contribute considerably to the measured flux levels of EPIC 210282472 and 210282473, increasing their brightnesses and lowering the amplitudes and photon noise levels we measure. Nevertheless, this zero-point uncertainty only changes the overall amplitudes and does not distort the shape of the light curves, and therefore has no further effect on the astrophysical content of the data.

For all three of these objects, the photometric magnitudes have been transformed into the USNO-B1.0 R system (Monet et al. 2003). This procedure was performed similar to that in Pál et al. (2015). The raw and processed photometric data series are displayed in Table 2. Note that the photometric errors shown in this table do not include the aforementioned zero-point uncertainty.

We carried out a standard Fourier analysis with the Period04 software (Lenz & Breger 2005), using multi-frequency least-squares fits and consecutive prewhitenings. The identified frequency components are listed in Table 3. We detected modulation triplets (nf_1 harmonics and corresponding $nf_1 \pm f_m$ side peaks, where $n = 1, 2, 3 ...$) in the Fourier spectra of EPIC 210282473 and 210282474. We note, however, that in the latter case, the length of the data is insufficient to properly resolve the side peaks and their distances correspond to the length of the data instead of the modulation period, so we did not include them in the fit.

We also could identify the characteristic signal of the spacecraft attitude correction maneuvers at $f_{\rm corr} = 4.08\ {\rm day}^{-1}$ and its harmonics, but with a signal-to-noise ratios (S/Ns) below 4. Apparently, very faint objects suffer less from the

Table 2
K2 Photometric Data of the RR Lyr Stars in Leo IV

Object	Time (BJD)	Brightness (R mag)[a]	Error (mag)	Type
210282472	2456810.28292	20.865	0.062	raw
210282472	2456810.30336	20.659	0.048	raw
210282472	2456810.32379	20.974	0.058	raw
210282473	2456810.28292	21.247	0.069	raw
210282473	2456810.30336	21.188	0.069	raw
210282473	2456810.32379	21.240	0.076	raw
210282474	2456810.28292	21.821	0.122	raw
210282474	2456810.30336	21.585	0.093	raw
210282474	2456810.32379	21.565	0.085	raw
210282472	2456810.28292	20.886	0.062	proc
210282472	2456810.32379	20.995	0.058	proc
210282472	2456810.34422	21.004	0.054	proc

Note.
[a] Magnitudes shown here are transformed to the USNO-B1.0 R system (see the text for further details). Indices "raw" and "proc" correspond to the raw and processed (sigma-clipped and Fourier-filtered) data, respectively.

(This table is available in its entirety in machine-readable form.)

Table 3
Frequency Tables for EPIC 210282472, 210282473, and 210282474

EPIC	Freq. ID	Freq (day^{-1})	Amp (mag)	ϕ (rad/2π)	$\pm F$ (day^{-1})	$\pm A$ (mag)	$\pm\phi$ (rad/2π)
210282472	f_0	1.40872	0.1400	0.1786	0.00011	0.0023	0.0024
	$2f_0$	2.81745	0.0640	0.7512	0.00023	0.0023	0.0053
	$3f_0$	4.22617	0.0427	0.380	0.00035	0.0023	0.008
	$4f_0$	5.6349	0.0217	0.999	0.0007	0.0020	0.016
	$5f_0$	7.0436	0.0106	0.679	0.0014	0.0019	0.032
210282473	f_0	1.61545	0.2249	0.1459	0.00008	0.0032	0.0017
	$2f_0$	3.23090	0.0869	0.6798	0.00020	0.0032	0.0045
	$3f_0$	4.84635	0.0616	0.2126	0.00028	0.0031	0.0064
	$4f_0$	6.46181	0.0405	0.801	0.00042	0.0031	0.010
	$5f_0$	8.0773	0.0265	0.349	0.0006	0.0030	0.015
	$6f_0$	9.6927	0.0152	0.950	0.0011	0.0028	0.026
	$f_0 - f_m$	1.5818	0.0261	0.016	0.0006	0.0025	0.015
	$f_0 + f_m$	1.6491	0.0150	0.344	0.0012	0.0031	0.029
	$2f_0 - f_m$	3.1973	0.0199	0.485	0.0008	0.0030	0.019
	$3f_0 - f_m$	4.8127	0.0132	0.998	0.0012	0.0030	0.028
	$4f_0 - f_m$	6.4282	0.0104	0.507	0.0016	0.0031	0.037
	$5f_0 - f_m$	8.0436	0.0119	0.144	0.0014	0.0031	0.033
	$5f_0 + f_m$	8.1109	0.0098	0.436	0.0018	0.0029	0.041
	$6f_0 + f_m$	9.7263	0.0095	0.097	0.0018	0.0029	0.043
210282474	f_0	1.58582	0.2899	0.7674	0.00007	0.0032	0.0017
	$2f_0$	3.17164	0.1219	0.9159	0.00018	0.0032	0.0041
	$3f_0$	4.75747	0.0846	0.0845	0.00025	0.0036	0.0058
	$4f_0$	6.34329	0.0553	0.300	0.00039	0.0035	0.009
	$5f_0$	7.9291	0.0313	0.516	0.0007	0.0035	0.016
	$6f_0$	9.5149	0.0136	0.677	0.0016	0.0035	0.036

Note. Frequencies, amplitudes, phases, and their respective uncertainties. The modulation frequency for EPIC 210282473 was set to $f_m = 0.03361$ day^{-1}.

attitude changes of K2 than bright targets. Other significant frequency peaks, such as low-amplitude additional modes or half-integer peaks related to period doubling—both observed in many modulated RRab stars—did not appear after prewhitening. This is not surprising, however, considering that the 3 S/N significance limit in the Fourier spectra is around 8–12 mmag, well above the strongest additional peaks detected in the original *Kepler* sample. The additional modes described by Benkő et al. (2014) reached only 3 mmag, and so similar modes would be undetectable in the Leo IV stars. The Fourier spectra of EPIC 210282473are shown in Figure 4.

Such faint targets are very sensitive to any instrumental problems arising both from the observations and the data reduction. Counterintuitively, the light curve of the only unblended star, EPIC 210282474, was the most problematic in our case. Even after Fourier filtering, some slow, low-amplitude (∼0.1 mag) variations still persisted in the last 15 days of the light curve (Figure 3). Examination of the K2 full-frame images did not reveal any obvious contaminating sources in the same or adjacent modules. The SDSS images did not reveal any nearby objects either (see Figure 2). We visually inspected the stacked image obtained using the observations taken with the 2.5 m Isaac Newton Telescope, the 4.2 m William Herschel Telescope, and the 4.1 m Southern Astrophysical Research Telescope in 2007 by Moretti et al. (2009), but found no significant nearby objects to within 1.″0. This image is displayed in Figure 1. Images of the other two targets indicate that the confusion is caused almost exclusively by a single bright galaxy near each star. Another star can be detected 2.″1 from 210282472, but it is about 3.5 mag fainter than the RR Lyrae target, so its contribution is negligible.

4. RESULTS

4.1. Blazhko Effect in Leo IV

One star, EPIC 210282473, is clearly modulated. Although signs of amplitude changes in RR Lyrae stars have been observed as far as the Andromeda galaxy (Brown et al. 2004), this is the first star beyond the Magellanic Clouds for which detailed modulation properties can be determined. The K2 data covers almost three Blazhko cycles. The distance of the triplet side peaks ($nf_1 \pm f_m$) suggested a modulation period of $P_m = 30 \pm 3$ day, but the independent fits to the modulation peaks resulted in large uncertainties. We also calculated the amplitude and phase variations (A_1, ϕ_1) of the main frequency peak (f_1) by dividing the data into short segments. A sine fit to $A_1(t)$ itself led to a more precise Blazhko period: $P_m = 29.8 \pm 0.9$ day.

Figure 5 shows the modulation properties of EPIC 210282473. The right panel is the light curve, folded with the modulation period: the presence of the Blazhko effect is even more clear here than in the normal light curve. The left panel illustrates how the shape of the light curve itself changes over a modulation cycle. We selected two 2-day long sections of a low- and a high-amplitude state, respectively, and calculated the phase-binned values of the data. Red squares and blue circles show the two states, respectively: the differences in amplitude are evident around maximum and

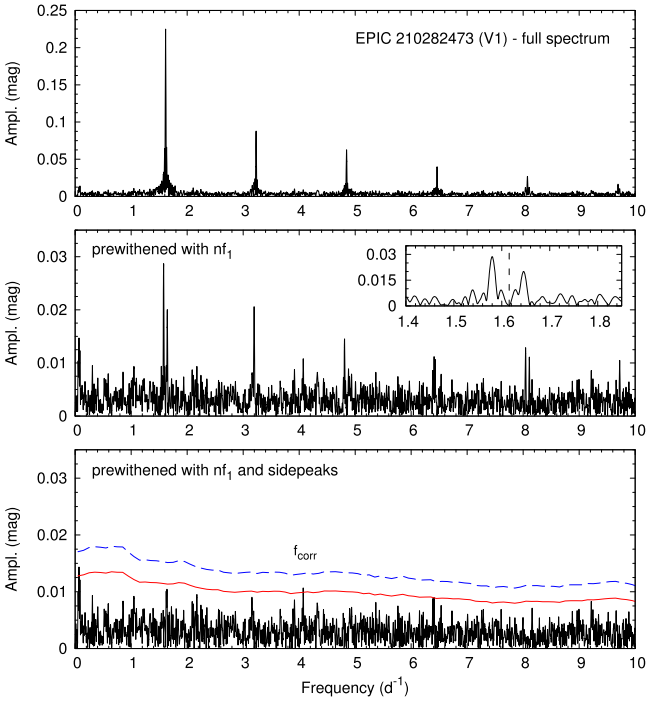


Figure 4. Fourier transform of the light curve of EPIC 210282473. The top panel shows the original spectrum. Significant modulation side peaks are visible in the middle panel after prewhitening with the main peak and its harmonics. The insert shows the triplet around the position of the main peak (dashed line). The bottom panel shows the residual after the side peaks have been prewhitened as well. The red solid and blue dashed lines are the 3 and 4 S/N levels, respectively. The $f_{\rm corr}$ label marks the position of the marginally detected spacecraft attitude correction frequency.

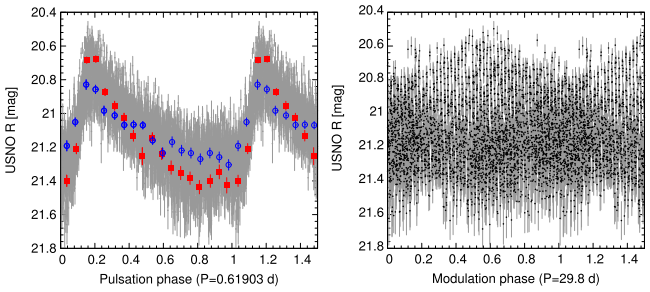


Figure 5. Blazhko effect in EPIC 210282473. Left: data folded with the pulsation period. Binned data from 2-day long sections are overlaid, red dots show the maximum-amplitude modulation phase, and blue circles show the minimum-amplitude phase. Right: light curve folded with the modulation period.

minimum light, but the phases at which the extrema occur show little to no shifts.

Another representation is included in Figure 6 where the upper and middle panels show the variation of the A_1 and ϕ_1 Fourier-terms. These figures confirm that there is significant amplitude variation in the data, but the phase modulation is almost negligible in the star. Moreover, the middle column of Figure 6 indicates that the cycles are not repetitive and the amplitude and phase variation are not strictly correlated to each other, similar to some modulated stars in the original *Kepler* sample (Benkő et al. 2014).

The case of EPIC 210282474 is more ambiguous, since the light curve of the star suffers from instrumental effects more than those of the other two. The Fourier-filtered light curve shows some amplitude and phase variation, but those are suspiciously—but not exactly—symmetric to the mid-campaign data download period. This symmetry in the amplitudes causes us to suspect some kind of instrumental origin, although we could not identify any contaminating source. We also detect weak phase variations that seem to follow the changes in the pulsation amplitude (right column of Figure 6). If we accept that these variations indeed originate from modulation, then its period is clearly longer than the length of the campaign. We identified side peaks in the frequency spectrum, but given the limited length of the data, they are not resolved properly. Overall, since we also detect variations in the first, better-quality part of the light curve, we accept this signal as a likely (although not unquestionable) detection of the Blazhko effect. Most stars in the Milky Way have modulation periods longer than 10–20 days (Szczygieł and Fabrycky 2007): the values we determined for the Leo IV stars agree with that period distribution. Although the Leo IV sample is very limited, it confirms that the Blazhko effect is abundant in other galaxies as well.

EPIC 210282472 also shows some phase variations but only marginal changes in amplitude (left column of Figure 6). However, these amplitude changes can be partly attributed to the large scatter of the light-curve points that make the phase determination uncertain for shorter data segments (10 days per segment in this case). Given the lack of significant amplitude variations, we classify this star as non-modulated.

We also calculated the Fourier phase values for the original observations of Moretti et al. (2009) with the frequencies determined from the K2 data, and transformed them to the more classical O–C diagrams. The results, shown in the bottom row of Figure 6, suggest that the pulsation period of EPIC 210282473 became shorter during the 7.1 years separating the two data sets, while the periods of EPIC 210282472 and 210282474 got longer. Other observations between the two epoch were too sparse to determine the pulsation phase and O–C values. Therefore, the actual rates of period change cannot yet be determined.

4.2. Photometric Metallicities

A great advantage of RR Lyrae stars is that we can estimate their [Fe/H] indices from photometry alone (Jurcsik and Kovács 1996). Nemec et al. (2013) have calibrated the relation between the light-curve parameters and the spectroscopically determined metallicity values for the *Kepler* passband and showed that the photometric and spectroscopic [Fe/H] indices agree to ± 0.1 dex for all but the extremely modulated stars. We calculated the photometric [Fe/H] values for all three stars with this method: the results are summarized in Table 4. The accuracy intrinsic to Fourier parameter determination is ± 0.03 dex. However, according to Nemec et al. (2013), the uncertainties of the relation are dominated by the calibration of the equation and the determination of the spectroscopic values, so we assumed higher uncertainties for all of the stars (Table 4).

Of the three stars, only EPIC 210282472 has a spectroscopically determined index, $[{\rm Fe/H}] = -2.03$ (Kirby et al. 2008), that is higher, but within the respective error bars, compared to our photometric index of -2.16 ± 0.10, assuming the same uncertainties. Moretti et al. (2009) determined the photometric metallicity for EPIC 210282473, but their result, $[{\rm Fe/H}] = -2.11$, is significantly higher than the K2-derived value (-2.64 ± 0.10). This discrepancy can largely be

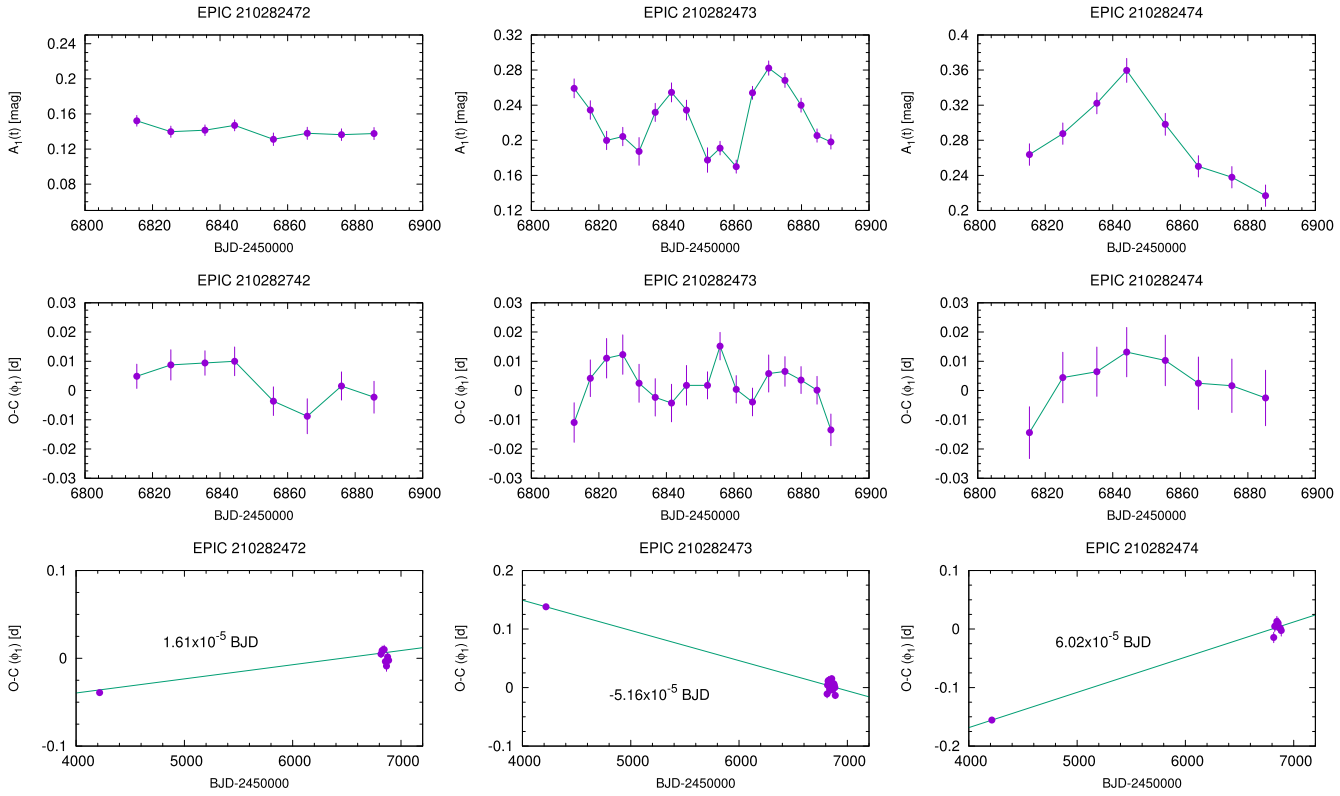


Figure 6. Top row: variation A_1, the amplitude of the f_1 frequency component in all three stars. Middle row: O–C variation, calculated as the variation of the ϕ_1 Fourier parameter. Bottom row: long-term period drifts of all three stars between 2007 (Moretti et al. 2009) and 2014, the K2 observations.

Table 4
Pulsation Periods, Modulation Periods, and Photometric [Fe/H] Indices of the RR Lyr Targets

Object	Pulsation per. (day)	Mod. per. (day)	[Fe/H]
472	$0.709862 \pm 5.5 \cdot 10^{-5}$	...	-2.16 ± 0.10
473	$0.619022 \pm 3.1 \cdot 10^{-5}$	29.8 ± 0.9	-2.64 ± 0.10
474	$0.630588 \pm 4.4 \cdot 10^{-5}$	>80	-2.62 ± 0.15

attributed to the fact that the linear relation of Jurcsik and Kovács (1996), used by Moretti et al. (2009), overestimates the [Fe/H] index by as much as ∼0.3 dex for very metal-poor stars. The K2 data also revealed that the star is modulated, and the poor modulation phase coverage may have affected the original metallicity determination. Since the Blazhko effect in the star is well covered by the K2 data and does not show extreme amplitude changes or cycle-to-cycle variability, we consider the photometric metallicity to be accurate to 0.10 dex (Nemec et al. 2013).

We calculated the metallicity of the third star, EPIC 210282474, to be [Fe/H] $= -2.62 \pm 0.15$. We note that if the star is indeed modulated, then the partial phase coverage of the Blazhko effect could affect the photometric metallicity value. We increased the uncertainty to account for this additional factor. Overall, the three metallicity values are in good agreement with the average metallicity values of Leo IV (around –2.3 or –2.6) and confirm its very metal-poor nature.

5. CONCLUSIONS

We detected the variations of all three extragalactic RR Lyrae stars in the K2 mission Campaign 1 data. The stars are members of the ultra-faint dwarf spheroidal galaxy Leo IV (Moretti et al. 2009). These are the faintest pulsating stars measured with the *Kepler* space telescope so far, at a brightness level of $Kp \approx 21.5$ mag.

One of the variables, EPIC 210282473, displays clear amplitude variations with a period of 29.8 ± 0.9 days, while EPIC 210282474 is likely modulated with a period longer than the campaign length (80 days). In the case of the former star, almost three modulation cycles are covered during which the strength of the Blazhko effect and the relation between the amplitude and phase modulation both changed. These observations are the farthest measurements of the detailed parameters of the Blazkho effect at a distance of 154 kpc, and the first beyond the Milky Way and the Magellanic Clouds. We determined the photometric [Fe/H] indices of the stars that range between –2.16 and –2.64, in agreement with the spectroscopic values measured in Leo IV.

We also demonstrated that with fine-tuned algorithms based on image subtraction, we can achieve nearly the same faintness level for stationary targets as is attainable for moving objects, such as TNOs. We found that unlike brighter sources, very faint but high-amplitude variations do not significantly contain frequencies caused by the attitude correction maneuvers of *Kepler*. The implications of this exercise are far-reaching, as photometric space missions will continue to stare at crowded fields in the future. Globular clusters have already been measured during the K2 mission, and *Kepler* may observe Cepheid stars in another galaxy, IC 1613, in Campaign 8. The TESS and PLATO missions will employ even larger pixels than *Kepler* did, leading to strong crowding in several fields where image subtraction will be a necessary requirement (Rauer et al. 2014; Ricker et al. 2014). One important example is the Large Magellanic Cloud within the southern continuous

observing zone of TESS. The LMC contains several bright, large-amplitude variables (Cepheids for example) that will be accessible for that mission, but their photometry will present challenges very similar to the K2 observations presented here in terms of crowding and signal-to-noise ratios.

We are grateful to the referee for constructive comments that helped to improve the paper. We thank the hospitality of the Veszprém Regional Centre of the Hungarian Academy of Sciences (MTA VEAB) where part of our work was carried out. Funding for the *Kepler* and K2 missions is provided by the NASA Science Mission directorate. The authors gratefully acknowledge the *Kepler* team, the Guest Observer Office, and Ball Aerospace, whose outstanding efforts have made these results possible. This project has been supported by the Lendület-2009, LP2012-31, and LP2014-17 Programs of the Hungarian Academy of Sciences and the Hungarian OTKA grants K-104607, and K-109276, and the NKFIH K-115709 grant of the Hungarian National Research, Development and Innovation Office. The research leading to these results has received funding from the ESA PECS Contract No. 4000110889/14/NL/NDe, and from the European Community's Seventh Framework Programme (FP7/2007-2013) under grant agreements No. 269194 (IRSES/ASK) and No. 312844 (SPACEINN). L.M. was supported by the János Bolyai Research Scholarship of the Hungarian Academy of Sciences. V.R. acknowledges partial support by the project PRIN-MIUR (2010LY5N2T) "Chemical and dynamical evolution of the Milky Way and Local Group galaxies" (P.I.: F. Matteucci). All of the data presented in this paper were obtained from the Mikulski Archive for Space Telescopes (MAST). STScI is operated by the Association of Universities for Research in Astronomy, Inc., under NASA contract NAS5-26555. Support for MAST for non-*HST* data is provided by the NASA Office of Space Science via grant NNX09AF08G and by other grants and contracts.

REFERENCES

Alcock, C., Allsman, R. A., Axelrod, T. S., et al. 1996, AJ, 111, 1146
Belokurov, V., Zucker, D. B., Evans, N. W., et al. 2007, ApJ, 654, 897
Benkő, J. M., Plachy, E., Szabó, R., Molnár, L., & Kolláth, Z. 2014, ApJS, 213, 31
Borucki, W. J., Koch, D., Basri, G., et al. 2010, Sci, 327, 977
Brown, T. M., Ferguson, H. C., Smith, E., et al. 2004, AJ, 127, 2738
Da Costa, G. S., Rejkuba, M., Jerjen, H., & Grebel, E. K. 2010, ApJL, 708, L121
Howell, S. B., Sobeck, C., Haas, M., et al. 2014, PASP, 126, 398
Jurcsik, H., & Kovács, G. 1996, A&A, 312, 111
Jurcsik, J., Sdor, Á, Szeidl, B., et al. 2009, MNRAS, 400, 1006
Kirby, E. N., Simon, J. D., Geha, M., Guhathakurta, P., & Frebel, A. 2008, ApJ, 685, 43
Lenz, P., & Breger, M. 2005, CoAst, 146, 53
Molnár, L., Szabó, R., Moskalik, P. A., et al. 2015, MNRAS, 452, 4283
Monet, D. G., Levine, S. E., Canzian, B., et al. 2003, AJ, 125, 984
Moretti, M. I., Dall'Ora, M., Ripepi, V., et al. 2009, ApJ, 699, 125
Nemec, J. M., Cohen, J. G., Ripepi, V., et al. 2013, ApJ, 773, 181
Olling, R. P., Mushotzky, R., Shaja, E. R., et al. 2015, Natur, 521, 332
Pál, A. 2009, arXiv:0906.3486
Pál, A. 2012, MNRAS, 421, 1825
Pál, A., Szabó, R., Szabó, Gy. M., et al. 2015, ApJL, 804, L45
Rauer, H., Catala, C., Aerts, C., et al. 2014, ExA, 38, 249
Ricker, G. R., Winn, J. N., Vanderspeck, R., et al. 2014, Proc. SPIE, 9143, 914320
Sand, D. J., Seth, A., Olszewski, E. W., et al. 2010, ApJ, 718, 530
Simon, J. D., & Geha, M. 2007, ApJ, 670, 313
Soszynski, I., Udalski, A., Szymanski, M., et al. 2009, AcA, 59, 1
Soszynski, I., Udalski, A., Szymanski, M., et al. 2014, AcA, 64, 177
Soszynski, I., Udalski, A., Szymanski, M. K., et al. 2010, AcA, 60, 165
Stetson, P. B., Fiorentino, G., Bono, G., et al. 2014, PASP, 126, 616
Szabó, R., Kolláth, Z., Molnár, L., et al. 2010, MNRAS, 409, 1244
Szabó, R., Sárneczky, K., Szabó, Gy. M., et al. 2015, AJ, 149, 112
Szczygieł, D. M., & Fabrycky, D. C. 2007, MNRAS, 377, 1263